Bistatic Radar Cross Sections of Chaff

PEYTON Z. PEEBLES, JR., Senior Member, IEEE
University of Florida

Bistatic cross sections applicable to scattering from a cloud of randomly positioned and randomly oriented resonant dipoles, or chaff, are found. The chaff cloud can have an arbitrary location relative to an illuminating radar and the radar antenna can have an arbitrarily specified polarization. The receiver can be located arbitrarily in relation to the radar and chaff cloud and can also have arbitrary polarization (different from the transmitter antenna). Average cross sections are found for a preferred receiver polarization and the corresponding orthogonal polarization. Results are reduced to simple, easily applied expressions, and several examples are developed to illustrate the ease with which the general results can be applied in practice.

Manuscript received July 22, 1983; revised November 7, 1983.

This work was supported by Harry Diamond Laboratories, United States Army, under Contract DAAK21-82-C-0107.

Author's address: Department of Electrical Engineering, University of Florida, Gainesville, FL 32611.

0018-9251/84/0300-0128 $1.00 © 1984 IEEE

I. INTRODUCTION

Chaff is a countermeasure designed to reduce the effectiveness of radar. It has also been used in communication systems. It usually consists of a large number of thin, highly conducting wires dispensed in the atmosphere to form a "cloud" of scatterers. Energy scattered by the cloud and received by a radar would ideally be large enough to mask the presence of some target the chaff is to protect. The strips may have many forms but typically are cut to a length so that they become resonant dipoles at the radar's frequency. The dipoles also will be effective at harmonics of the radar frequency. For example, dipoles that are tuned to half-wavelength resonance at frequency f_0 will be full-wave dipoles at $2f_0$, three-halves wavelength at $3f_0$, etc. By dispensing dipoles of several lengths, chaff can be made effective over a wide band of frequencies.

Chaff was first used in World War II to confuse German radar, but it remains an important countermeasure to date. Many parameters enter into the overall effectiveness of chaff, such as physical cross sectional area of chaff elements (dipoles), losses in the elements, speed and extent to which clouds form, effects of winds and turbulence on dipole shape, fall speed, and attitudes of the elements, weight, volume, clustering (birdnesting) tendencies, and radar cross section. This paper is concerned only with the radar cross section of chaff. For the reader interested in the other parameters, several survey papers are available [1–5].

The literature related to scattering from chaff and from chaff elements is voluminous and no effort will be made to give a comprehensive list of references. For a good listing of articles prior to about 1970, [6] is a good source. Reference [7] is a bibliography on the subject up to about 1983. We shall, however, cite a few references that are considered representative of the developments that have evolved and that relate most directly to the interests of this paper.

Early efforts to describe chaff effects centered mainly on *backscatter* cross section (monostatic scattering). Bloch et al. [8] gave one of the earliest analyses based on a simple, infinitely conducting, wire model of the dipole; backscatter cross section was found for a dipole element having any orientation relative to the incident wave. In addition, the importance of the randomness of dipole positions and orientations was realized and *average* cross sections were determined. For chaff elements with directions uniformly distributed over the sphere, the cross section was found to be $0.158\lambda^2$ per dipole, a value that is still representative. For dipoles in the wave's polarization plane, but uniformly distributed in angle within the plane, the cross section per dipole was found to be $0.289\lambda^2$ [8].

Apparently using a dipole model similar to [8], Chu, in unpublished work cited in [9], found the spherically averaged backscatter cross section, denoted by $\overline{\sigma}$, for *resonant* dipoles. His result can be put in the form

$$\overline{\sigma}/\lambda^2 = \frac{1.178(L/\lambda) - 0.131 + 0.179\ln(22.368\,L/\lambda)}{[\ln(22.368\,L/\lambda)]^2} \tag{1}$$

per dipole, where L is the dipole length, λ is wavelength, and L must be a multiple of $\lambda/2$, i.e., $L = M\lambda/2$, $M = 1,2,\ldots$. From (1), $\overline{\sigma} = 0.153\lambda^2$, $0.166\lambda^2$, and $0.184\lambda^2$ for half-wave, full-wave, and 1.5-wave dipoles, respectively.

Much effort has been made over the years to refine and extend the models for dipole scattering. One model based on induced electromotive force (EMF) was developed in [9]; it was called Method A and gave nearly the same results as Chu but was also valid for dipole lengths between resonances and nonzero wire cross sectional area. A second Method B [9] produced better agreement with measured data than Method A and was a first-order integral equation solution. Method B was comparable with an independent development of King and Middleton [10]. Another model due to Tai [11] applied to infinitely conducting dipoles and used a variational method. Cassedy and Fainberg [12] extended the model of Tai to include finite dipole conductivity. Harrison and Heinz [13] have considered backscatter for tubular and strip chaff elements as well as solid wires, all for finite conductivity. A model based on the Wiener–Hopf technique introduced by Chen [14] for thin wires applies to longer dipoles and appears to fit experimental data better than some earlier models. More complicated computer models taking into account mutual coupling between dipoles in a cloud are described by Wickliff and Garbacz [15]. Medgyesi-Mitschang and Eftimiu [16] have used Galerkin expansions to examine backscattering from infinitely conducting tubes. Other characteristics that have been studied that are applicable to backscatter from chaff are statistical properties [17] and spectral properties due to dipole motion [18, 19].

Whereas considerable effort has been made to describe backscattering, less effort has been made in the more general bistatic scattering problem. One of the earliest studies appears to be that of Hessemer [20] where reflections from chaff were used for communications. Useful formulas were derived for average cross sections assuming both spherical and planar random dipole distributions when using a simple thin wire model (similar to [8]). Mack and Reiffen [21] also used a thin wire model to find average bistatic cross sections and showed how they depend on linear or circular polarization. Some discussion of the effect of losses was also given. Unfortunately, there has been some question as to correctness of some results in [21] as pointed out by Harrington [22]. We say more about this below. Borison [23] has also obtained some specific average cross sections, but only for linear polarizations. Other studies of bistatic scattering from dipoles [24–29] have used more exact models, but results obtained are either somewhat difficult to apply in practical cases, do not give explicit equations for cross section useful to applications, or do not show the way in which geometry and polarizations of transmit and receive antennas affect the scattering. Some of these efforts also did not obtain the averaged cross section of chaff.

Probably the most complete study of chaff to date is due to Dedrick et al. [30]. By applying an approach using Stokes parameters they were able to show that four independent quantities are all that are required to determine any chaff cross section. The results in [30] applied to any combination of transmit–receive antenna polarizations, but how to compute results for such combinations was not shown. Results that were given were mainly in the form of graphs derived from simulations and these were for dipole lengths that are not usually of much interest in practice (no specific equations were given for solutions of the four required parameters).

The most recent analyses of bistatic chaff have used the polarization scattering matrix. Heath [31] has used this approach to show the relations between cross sections applicable to circular transmit–receive polarizations and cross sections applicable to linear field components parallel and normal to the plane containing transmitter, scatterer, and receiver. Other work [32] showed the relationship between circular cross sections and cross sections applicable to linear transmit–receive polarizations.

From the above discussion one concludes that the complete solution to the problem of bistatic scattering from chaff, even for the simple dipole model, has not been developed. It is the purpose of this paper to present such a solution in a form that is readily applied in practice. Specifically, we shall determine explicit equations for the chaff bistatic cross section presented to a receiving antenna having arbitrary (elliptical) polarization, arbitrary location, and viewing the chaff cloud in an arbitrary direction when that cloud is being illuminated by a transmitter having an arbitrarily polarized (different elliptical) antenna. Our results are in a form that is easy to use, and several specific examples of practical interest are developed in detail.

II. PROBLEM DEFINITION AND SUMMARY OF RESULTS

A. Problem Definition

The overall geometry applicable to bistatic scattering is shown in Fig. 1. A transmit antenna located at point T radiates an arbitrarily polarized wave toward a cloud of randomly positioned and randomly oriented dipoles represented by point D.[1] The transmit direction is defined by spherical coordinate angles θ_1, ϕ_1 defined in the common x,y,z coordinate frame. The dipole cloud is assumed far enough away that the incident wave is planar. Cloud extent is assumed to be small enough in relation to average distance, denoted by r_1, so that

[1]Clearly, point D cannot represent the cloud; it is helpful to view D as a point toward which both transmit and receiver antennas are directed and about which dipoles in the cloud are dispersed.

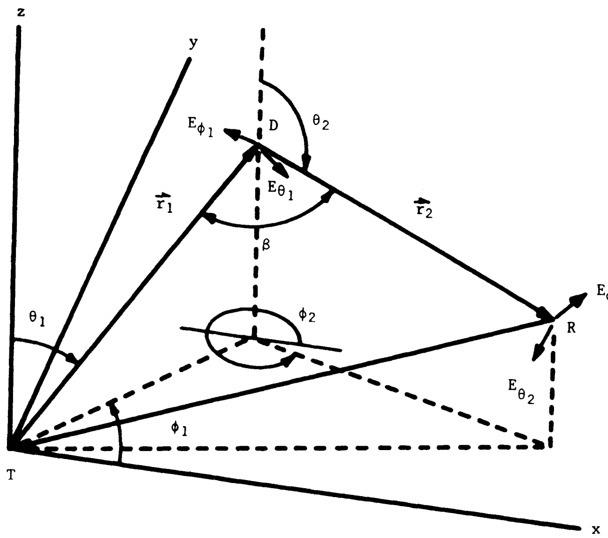

Fig. 1. Overall geometry of bistatic scattering.

strength of the incident field is approximately the same for all dipoles.

Scattering between dipoles is assumed negligible and dipoles are presumed sufficiently dispersed that mutual coupling is of no concern. Study has shown [29] that dipoles spaced at least two wavelengths apart in any direction produce almost no mutual coupling; average spacings down to 0.4λ, where λ denotes wavelength, can produce up to 3 dB loss in bistatic cross section. Dipoles are assumed to be infinitely conducting wires with a length that produces resonance at the transmitter frequency; thus we shall assume the simple wire model. In many practical cases dipole size and material are such that dipole losses are negligible [33].

As illustrated in Fig. 1 a typical dipole scatters some energy in the direction of a receiver, at point R, defined by spherical angles θ_2, ϕ_2. The receiving antenna is assumed far enough away from all dipoles in the cloud being viewed by the receiver antenna so that all dipole–receiver path distances approximately equal the average distance, denoted by r_2. The receiver is arbitrarily located and the angle between its line of sight (RD) and the radar's line of sight (TD) is called the bistatic scattering angle, denoted by β.

Both transmit and receive antennas are presumed to be arbitrary, that is, they are elliptically polarized. By employing the usual complex envelope representation of fields, the transmitted (or received) field polarization can be defined by a complex quantity Q (Q_T for transmitters, Q_R for receiver) that equals the complex field in the ϕ direction (ϕ_1 for transmitter; ϕ_2 for receiver) divided by the complex field in the θ direction (θ_1 for transmitter; θ_2 for receiver). Appendix A gives details on ways of selecting Q_T and Q_R for specific systems. The electric field of the wave incident on the dipole cloud is denoted by $\boldsymbol{E}_1$; it has components in directions θ_1 and ϕ_1 and its polarization is determined by Q_T. The electric field vector, denoted by $\boldsymbol{E}_2$, of the wave arriving at the receiver can be decomposed into the sum of an electric field vector, denoted by $\boldsymbol{E}_{R_1}$, of an elliptically polarized wave having the receive antenna's polarization, defined by Q_R, and a second wave's electric field vector, denoted by $\boldsymbol{E}_{R_2}$, having the orthogonal polarization also defined by Q_R.

With the above definitions we define bistatic cross section, denoted by σ, based on the power arriving at the receiver in the receiver's preferred polarization according to

$$\sigma = \lim_{r_2 \to \infty} 4\pi r_2^2 \left(|\boldsymbol{E}_{R_1}|^2/|\boldsymbol{E}_1|^2\right) \approx 4\pi r_2^2 |\boldsymbol{E}_{R_1}|^2/|\boldsymbol{E}_1|^2. \tag{2}$$

Cross section, denoted by σ_x, can also be defined for power arriving at the receiver in the orthogonal polarization by

$$\sigma_x = \lim_{r_2 \to \infty} 4\pi r_2^2 \left(|\boldsymbol{E}_{R_2}|^2/|\boldsymbol{E}_1|^2\right) \approx 4\pi r_2^2 |\boldsymbol{E}_{R_2}|^2/|\boldsymbol{E}_1|^2. \tag{3}$$

The approximations in (2) and (3) are true because we have assumed r_2 relatively large. These cross sections depend on the exact dipole positions and orientations. A reasonable approach to reducing the complexity of (2) and (3) is to take advantage of the random nature of positions and orientations by treating these quantities as random variables and averaging to get average cross sections, denoted by $\overline{\sigma}$ and $\overline{\sigma}_x$. By using $E[\cdot]$ to denote the statistical average we have

$$\overline{\sigma} = 4\pi r_2^2 E[|\boldsymbol{E}_{R_1}|^2]/|\boldsymbol{E}_1|^2 \tag{4}$$

$$\overline{\sigma}_x = 4\pi r_2^2 E[|\boldsymbol{E}_{R_2}|^2]/|\boldsymbol{E}_1|^2. \tag{5}$$

B. Summary of Results

In the following sections we show that

$$\overline{\sigma} = \frac{N}{(1+|Q_T|^2)(1+|Q_R|^2)} \Big\{ (\overline{\sigma}_{\perp \text{ to } \perp}|W_1|^2 + \overline{\sigma}_{\perp \text{ to } \parallel}|W_2|^2)|X_1|^2 + (\overline{\sigma}_{\perp \text{ to } \parallel}|W_1|^2 + \overline{\sigma}_{\parallel \text{ to } \parallel}|W_2|^2)|X_2|^2 + 4\overline{\sigma}_\Delta \operatorname{Re}(W_1 W_2^*)\operatorname{Re}(X_1 X_2^*) \Big\} \tag{6}$$

$$\overline{\sigma}_x = \frac{N}{(1+|Q_T|^2)(1+|Q_R|^2)} \Big\{ (\overline{\sigma}_{\perp \text{ to } \perp}|W_2|^2 + \overline{\sigma}_{\perp \text{ to } \parallel}|W_1|^2)|X_1|^2 + (\overline{\sigma}_{\perp \text{ to } \parallel}|W_2|^2 + \overline{\sigma}_{\parallel \text{ to } \parallel}|W_1|^2)|X_2|^2 - 4\overline{\sigma}_\Delta \operatorname{Re}(W_1 W_2^*)\operatorname{Re}(X_1 X_2^*) \Big\} \tag{7}$$

where $\operatorname{Re}(\cdot)$ represents the real part of the quantity in parentheses, the asterisk denotes complex conjugation, and

$$X_1 = T_1 - T_2 Q_T \tag{8}$$

$$X_2 = T_2 + T_1 Q_T \quad (9)$$

$$T_1 = \sin\theta_2 \sin(\phi_1 - \phi_2)/\sin\beta \quad (10)$$

$$T_2 = [\sin\theta_1 \cos\theta_2 - \cos\theta_1 \sin\theta_2 \cos(\phi_1 - \phi_2)]/\sin\beta \quad (11)$$

$$W_1 = R_1 - R_2 Q_R \quad (12)$$

$$W_2 = R_2 + R_1 Q_R \quad (13)$$

$$R_1 = \sin\theta_1 \sin(\phi_1 - \phi_2)/\sin\beta \quad (14)$$

$$R_2 = -[\sin\theta_2 \cos\theta_1 - \cos\theta_2 \sin\theta_1 \cos(\phi_1 - \phi_2)]/\sin\beta. \quad (15)$$

N is the number of dipoles being illuminated by the transmitter that exists in the volume viewed by the receiver's antenna, and $\bar{\sigma}_{\perp \text{ to } \perp}$, $\bar{\sigma}_{\parallel \text{ to } \parallel}$, $\bar{\sigma}_{\perp \text{ to } \parallel}$, and $\bar{\sigma}_{\Delta}$ are four functions (actually cross sections) that are defined and graphed (Figs. 3–6) in the subsequent text. It results that these four functions depend only on β (for a given dipole length) and are independent of other scattering geometry involving r_1, θ_1, ϕ_1, r_2, θ_2, and ϕ_2.

For a given problem where the geometry is given such that r_1, θ_1, ϕ_1, r_2, θ_2, ϕ_2, β, N, and λ are known, the use of (6) and (7) involves mainly two things. First, for whatever dipole case is of interest, the functions $\bar{\sigma}_{\perp \text{ to } \perp}$, $\bar{\sigma}_{\parallel \text{ to } \parallel}$, $\bar{\sigma}_{\perp \text{ to } \parallel}$, and $\bar{\sigma}_{\Delta}$ are determined from the graphs given. Second, Q_T and Q_R must be specified for the transmitter and receiver. Table I is helpful in choosing the Qs for the more common cases. In the general case of elliptical polarizations the relationships of the Appendix may be used.

TABLE I
Values of Q for various wave polarization

Wave Polarization	Q	A	B	α
Linear in θ direction	0	arbitrary $\neq 0$	0	0
Linear in ϕ direction	∞	0	arbitrary $\neq 0$	0
Linear tilted by angle ϕ_0 from ϕ axis	$\cot\phi_0$	arbitrary	$A\cot\phi_0$	0
Left circular	j	arbitrary	$= A$	$\pi/2$
Right circular	$-j$	arbitrary	$= A$	$-\pi/2$

III. ANALYSIS OF SINGLE DIPOLE SCATTERING

The overall scattering geometry is given in Fig. 1. By proper choise of coordinates defining scattering by the dipole at point D, the effect of the dipole can be separated from the incident path parameters r_1, θ_1, ϕ_1, and the scattering path parameters r_2, θ_2, and ϕ_2. The choice consists of defining a scattering plane TDR. The scattering plane and dipole geometry are shown in Fig. 2. A coordinate system x', y', z' is defined such that x' and y' axes lie in the plane TDR with x' positioned to bisect the scattering angle β. The dipole is located at the origin of the primed coordinate system with its wire axis located by spherical angles θ_d and ϕ_d, as shown.

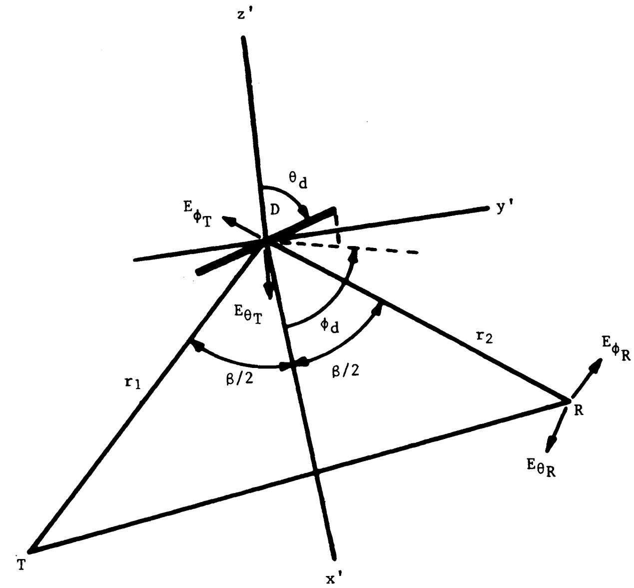

Fig. 2. Scattering plane and dipole geometry.

We define E_{ϕ_T} and E_{ϕ_R} as incident and received electric field components that lie in the scattering plane and are normal to axes TD and DR, respectively. Similarly we define field components E_{θ_T} and E_{θ_R} that are normal to the scattering plane and orthogonal to E_{ϕ_T} and E_{ϕ_R}, respectively, all as shown in Fig. 2. By using the polarization scattering matrix approach to the scattering problem we have

$$\begin{bmatrix} E_{\theta_R} \\ E_{\phi_R} \end{bmatrix} = \begin{bmatrix} d_{11} & d_{12} \\ d_{21} & d_{22} \end{bmatrix} \begin{bmatrix} E_{\theta_T} \\ E_{\phi_T} \end{bmatrix} = [d] \begin{bmatrix} E_{\theta_T} \\ E_{\phi_T} \end{bmatrix}. \quad (16)$$

Here $[d]$ is the scattering matrix of the dipole with elements d_{mn}, m and $n = 1, 2$, that are to be determined.

The field components E_{θ_T} and E_{ϕ_T} are related to the transmitted fields E_{θ_1} and E_{ϕ_1} (Fig. 1) that are incident on the dipole by

$$\begin{bmatrix} E_{\theta_T} \\ E_{\phi_T} \end{bmatrix} = \begin{bmatrix} T_{11} & T_{12} \\ T_{21} & T_{22} \end{bmatrix} \begin{bmatrix} E_{\theta_1} \\ E_{\phi_1} \end{bmatrix} = [T] \begin{bmatrix} E_{\theta_1} \\ E_{\phi_1} \end{bmatrix} \quad (17)$$

where $[T]$ is a field transformation matrix for the incident path that we subsequently determine. In an analogous manner, fields E_{θ_2} and E_{ϕ_2} (Fig. 1) at the receiver are related to E_{θ_R} and E_{ϕ_R} by

$$\begin{bmatrix} E_{\theta_2} \\ E_{\phi_2} \end{bmatrix} = \begin{bmatrix} R_{11} & R_{12} \\ R_{21} & R_{22} \end{bmatrix} \begin{bmatrix} E_{\theta_R} \\ E_{\phi_R} \end{bmatrix} = [R] \begin{bmatrix} E_{\theta_R} \\ E_{\phi_R} \end{bmatrix} \quad (18)$$

where $[R]$ is another field transformation matrix for the receiver path. By combining (16)–(18) we have

$$\begin{bmatrix} E_{\theta_2} \\ E_{\phi_2} \end{bmatrix} = [R]\,[d]\,[T] \begin{bmatrix} E_{\theta_1} \\ E_{\phi_1} \end{bmatrix}. \quad (19)$$

It is shown in the Appendix that the received wave can be decomposed into two elliptically polarized waves. One with electric field vector we denote by $\boldsymbol{E}_{R_1}$, will have an "amplitude" denoted by E_{R_1} and polarization set by Q_R which is that of the receiver antenna's polarization. The second wave, with electric field vector denoted by $\boldsymbol{E}_{R_2}$, has the polarization orthogonal to that of the receiver. Thus, from the Appendix, we write

$$\begin{bmatrix} E_{\theta_2} \\ E_{\phi_2} \end{bmatrix} = \boldsymbol{E}_{R_1} + \boldsymbol{E}_{R_2} = \begin{bmatrix} E_{R_1} \\ E_{R_1} Q_R \end{bmatrix} + \begin{bmatrix} -E_{R_2} Q_R^* \\ E_{R_2} \end{bmatrix}. \tag{20}$$

In a similar manner the transmitted wave's electric field vector, denoted by $\boldsymbol{E}_1$, incident at the dipole can be written as

$$\boldsymbol{E}_1 = \begin{bmatrix} E_{\theta_1} \\ E_{\phi_1} \end{bmatrix} = \begin{bmatrix} E_T \\ E_T Q_T \end{bmatrix} \tag{21}$$

where its "amplitude" is[2] E_T and its polarization is determined by Q_T.

By combining (20) and (21) with (19) we have

$$\begin{bmatrix} E_{R_1} \\ E_{R_2} \end{bmatrix} = \frac{1}{1 + |Q_R|^2} \begin{bmatrix} 1 & Q_R^* \\ -Q_R & 1 \end{bmatrix} [R]\,[d]\,[T] \begin{bmatrix} 1 \\ Q_T \end{bmatrix} E_T. \tag{22}$$

From the Appendix the power in the received fields in the antenna's preferred polarization is proportional to $|\boldsymbol{E}_{R_1}|^2 = (1 + |Q_R|^2)|E_{R_1}|^2$; the corresponding result for the orthogonal wave is $|\boldsymbol{E}_{R_2}|^2 = (1 + |Q_R|^2)|E_{R_2}|^2$. At the dipole, power in the incident wave is proportional to $|\boldsymbol{E}_1|^2 = (1 + |Q_T|^2)|E_T|^2$. From (4) and (5), cross sections become

$$\bar{\sigma} = \frac{4\pi r_2^2 (1 + |Q_R|^2)}{(1 + |Q_T|^2)} \frac{E[|E_{R_1}|^2]}{|E_T|^2} \tag{23}$$

$$\bar{\sigma}_x = \frac{4\pi r_2^2 (1 + |Q_R|^2)}{(1 + |Q_T|^2)} \frac{E[|E_{R_2}|^2]}{|E_T|^2}. \tag{24}$$

Thus by solving (22) we obtain average bistatic cross sections from (23) and (24); its solution requires that we first determine matrices $[R]$, $[T]$, and $[d]$.

A. Determination of Matrices [R] and [T]

Although we shall omit details because the procedures are straightforward, it is relatively easy to show that

$$[T] = \begin{bmatrix} T_1 & -T_2 \\ T_2 & T_1 \end{bmatrix} \tag{25}$$

where

$$T_1 = \sin\theta_2 \sin(\phi_1 - \phi_2)/\sin\beta \tag{26}$$

$$T_2 = [\sin\theta_1 \cos\theta_2 - \cos\theta_1 \sin\theta_2 \cos(\phi_1 - \phi_2)]/\sin\beta \tag{27}$$

and

$$[R] = \begin{bmatrix} R_1 & R_2 \\ -R_2 & R_1 \end{bmatrix} \tag{28}$$

where

$$R_1 = \sin\theta_1 \sin(\phi_1 - \phi_2)/\sin\beta \tag{29}$$

$$R_2 = -[\sin\theta_2 \cos\theta_1 - \cos\theta_2 \sin\theta_1 \cos(\phi_1 - \phi_2)]/\sin\beta. \tag{30}$$

B. Dipole Scattering Matrix [d]

Let the dipole be located as shown in the primed coordinate system of Fig. 2. Let θ and ϕ be angles in spherical coordinates locating an arbitrary direction of interest. Then for a dipole with a sinusoidal current distribution with current I_T in its center (terminal area if it were a center-fed dipole) the effective lengths in directions θ and ϕ, denoted by h_θ and h_ϕ, are known [35] to be

$$[h_\theta \quad h_\phi] = A(\theta, \phi)\,[-\sin\theta \cos\theta_d + \cos\theta \sin\theta_d \cos(\phi - \phi_d) \quad \sin\theta_d \sin(\phi_d - \phi)] \tag{31}$$

where we define

$$A(\theta, \phi) \triangleq \frac{(\lambda/\pi)}{\sin(\pi L/\lambda)} \frac{\cos[(\pi L/\lambda)\cos\psi] - \cos(\pi L/\lambda)}{\sin^2\psi} \tag{32}$$

and

$$\cos\psi = \cos\theta \cos\theta_d + \sin\theta \sin\theta_d \cos(\phi - \phi_d). \tag{33}$$

For the special definition of coordinates we employ, the two directions of interest, toward the receiver and toward the transmitter, lie in the x', y' plane so $\theta = \pi/2$ and we have

$$[h_\theta \quad h_\phi] = A(\pi/2, \phi)\,[-\cos\theta_d \qquad \sin\theta_d \sin(\phi_d - \phi)] \tag{34}$$

where

$$\cos\psi = \sin\theta_d \cos(\phi - \phi_d). \tag{35}$$

For a radiating dipole the electric fields are also known [35, p. 15]. Our dipole radiates toward point R located at $(r_2, \pi/2, \beta/2)$ from Fig. 2. The fields at point R become

$$\begin{bmatrix} E_{\theta_R} \\ E_{\phi_R} \end{bmatrix} = \frac{-j\eta I_T}{2\lambda r_2} \exp(-j2\pi r_2/\lambda) \begin{bmatrix} h_\theta(\pi/2, \beta/2) \\ h_\phi(\pi/2, \beta/2) \end{bmatrix} \tag{36}$$

[2] E_T is a complex "amplitude" and contains a factor $\exp(-j2\pi r_1/\lambda)$ which accounts for incident-path phase.

where $\eta = 120\,\pi$ is the intrinsic impedance of our medium, considered the same as free space. The radiated fields are due to the current induced into the dipole by the incident field. This current is the ratio of induced open-circuit equivalent voltage, denoted by V_{oc}, to antenna impedance, denoted by z_{rad}, when the load on the antenna as a receiver is zero (shorted dipole). We have

$$I_T = V_{oc}/z_{rad} = [E_{\theta_T} h_\theta(\pi/2, -\beta/2) - E_{\phi_T} h_\phi(\pi/2, -\beta/2)]/z_{rad}. \quad (37)$$

By combining (37) and (36) and writing the result in the form of (16), we have the elements of $[d]$

$$d_{11} = BA_0(\beta/2)\cos^2\theta_d \quad (38a)$$

$$d_{12} = BA_0(\beta/2)\cos\theta_d \sin\theta_d \sin(\phi_d + \beta/2) \quad (38b)$$

$$d_{21} = -BA_0(\beta/2)\cos\theta_d \sin\theta_d \sin(\phi_d - \beta/2) \quad (38c)$$

$$d_{22} = -BA_0(\beta/2)\sin^2\theta_d \sin(\phi_d - \beta/2) \sin(\phi_d + \beta/2) \quad (38d)$$

where we define

$$B \triangleq [-j\eta/(2\lambda z_{rad} r_2)] \exp(-j2\pi r_2/\lambda) \quad (39)$$

$$A_0(\beta/2) \triangleq A(\pi/2, \beta/2) A(\pi/2, -\beta/2). \quad (40)$$

C. Bistatic Cross Sections

Average cross sections can now be found from (23) and (24) using (22) since matrices $[R]$, $[T]$, and $[d]$ are now defined. Considerable detail is involved, so only the procedure is outlined. If we define two matrices according to

$$[X] = \begin{bmatrix} X_1 \\ X_2 \end{bmatrix} = \begin{bmatrix} T_1 - T_2 Q_T \\ T_2 + T_1 Q_T \end{bmatrix} \quad (41)$$

and

$$[W] = \begin{bmatrix} W_1 \\ W_2 \end{bmatrix} = \begin{bmatrix} R_1 - R_2 Q_R \\ R_2 + R_1 Q_R \end{bmatrix} \quad (42)$$

then E_{R_1} from (22) becomes

$$E_{R_1} = \frac{E_T}{1 + |Q_R|^2} [W^*]^t [d]\,[X]. \quad (43)$$

Here $[\cdot]^t$ denotes the matrix transpose.

By forming $|E_{R_1}|^2$ using (43) and expanding out the matrices, the result is a linear sum of terms involving all possible combinations of the coefficients of $[d]$ with themselves conjugated. When the average $E[|E_{R_1}|^2]$ is formed, assuming angles θ_d and ϕ_d are uniformly distributed in direction over the sphere, the following averages of the coefficient products result:

$$E[d_{11}d_{11}^*] \neq 0 \quad (44a)$$

$$E[d_{11}d_{12}^*] = E[d_{12}d_{11}^*] = 0 \quad (44b)$$

$$E[d_{11}d_{21}^*] = E[d_{21}d_{11}^*] = 0 \quad (44c)$$

$$E[d_{11}d_{22}^*] = E[d_{22}d_{11}^*] = E[d_{12}d_{21}^*] = E[d_{21}d_{12}^*] \neq 0 \quad (44d)$$

$$E[d_{12}d_{12}^*] = E[d_{21}d_{21}^*] \neq 0 \quad (44e)$$

$$E[d_{12}d_{22}^*] = E[d_{22}d_{12}^*] = 0 \quad (44f)$$

$$E[d_{21}d_{22}^*] = E[d_{22}d_{21}^*] = 0 \quad (44g)$$

$$E[d_{22}d_{22}^*] \neq 0. \quad (44h)$$

The four nonzero quantities in (44) are summarized below with appropriate symbol definitions

$$\bar\sigma_{\perp \text{ to } \perp} \triangleq 4\pi r_2^2 E[d_{11}d_{11}^*] = 4\pi r_2^2 |B|^2 E[A_0^2(\theta_d, \phi_d)\cos^4\theta_d] \quad (45)$$

$$\bar\sigma_{\perp \text{ to } \parallel} \triangleq 4\pi r_2^2 E[d_{12}d_{12}^*] = 4\pi r_2^2 |B|^2 E[A_0^2(\theta_d, \phi_d)\cos^2\theta_d \sin^2\theta_d \sin^2(\phi_d + \beta/2)] \quad (46)$$

$$\bar\sigma_\Delta \triangleq 4\pi r_2^2 E[d_{11}d_{22}^*] = -4\pi r_2^2 |B|^2 E[A_0^2(\theta_d, \phi_d)\cos^2\theta_d \sin^2\theta_d \sin(\phi_d - \beta/2)\sin(\phi_d + \beta/2)] \quad (47)$$

$$\bar\sigma_{\parallel \text{ to } \parallel} \triangleq 4\pi r_2^2 E[d_{22}d_{22}^*] = 4\pi r_2^2 |B|^2 E[A_0^2(\theta_d, \phi_d)\sin^4\theta_d \sin^2(\phi_d - \beta/2)\sin^2(\phi_d + \beta/2)] \quad (48)$$

where the spherical average is defined by

$$E[\cdot] = \frac{1}{4\pi}\int_{\phi_d=0}^{2\pi}\int_{\theta_d=0}^{\pi} [\cdot]\sin\theta_d\, d\theta_d d\phi_d. \quad (49)$$

With these definitions, $E[|E_{R_1}|^2]$ from (43) reduces to a reasonable number of terms, and when substituted into (23) we finally obtain the cross section $\bar\sigma$; it equals (6) with N set equal to unity.

By repeating the above procedure, the average bistatic cross section $\bar\sigma_x$ for the orthogonal receiver polarization is obtained; it is equal to (7) with N set equal to unity.

The use of (6) and (7) in a given problem amounts to use of specified transmitter and receiver antenna polarizations (determines Q_T and Q_R), specified geometry (determines X_1, X_2, W_1, and W_2), and finding the functions $\bar\sigma_{\perp \text{ to } \perp}$, $\bar\sigma_{\perp \text{ to } \parallel}$, $\bar\sigma_\Delta$, and $\bar\sigma_{\parallel \text{ to } \parallel}$. We next determine these functions.

D. Scattering Plane Cross Sections

It is easy to show that if transmitter, dipole, and receiver all lie in the x,y plane of Fig. 1, then $\bar{\sigma}_{\perp \text{ to } \perp}$ is the bistatic cross section when both transmitter and receiver antennas have linear polarization perpendicular to the scattering plane. Similarly, $\bar{\sigma}_{\parallel \text{ to } \parallel}$ applies when both are linear and parallel to the scattering plane, while $\bar{\sigma}_{\perp \text{ to } \parallel}$ is the cross section when both are linear with one parallel and the other perpendicular. Which is which in the last case is not important since it can be shown that $\bar{\sigma}_{\perp \text{ to } \parallel} = \bar{\sigma}_{\parallel \text{ to } \perp}$. We also show below that $\bar{\sigma}_{\Delta}$ is one-half of the difference between $\bar{\sigma}$ and $\bar{\sigma}_x$ when the transmitter and preferred receiver polarizations are linear and tilted 45° from the horizontal axis.

Since the four cross sections given by (45)–(48) are difficult to analytically solve in general, it is fortunate that they depend only on β and the dipole's length relative to λ.[3] This fact allows (45)–48) to be computed by digital computer for various values of β for selected dipole lengths and the results used for any general scattering problem through (6) and (7). Computed results are plotted in Figs. 3–6 for dipoles of resonant lengths of $\lambda/2$, λ, and $3\lambda/2$. The numerical data used in the plots are given in [36]. Four $L = \lambda/2$ the well-known value $z_{\text{rad}} = 73.0$ Ω was used. For $L = 3\lambda/2$ the impedance procedure of Kraus [34, p. 143] was extended to obtain $z_{\text{rad}} = 105.4$ Ω. For $L = \lambda$ our model contains an indeterminate form since $\sin(\pi L/\lambda) = 0$ in (32) while $z_{\text{rad}} = \infty$ in (37), theoretically; in this case it is reasonable that the form of the scattering determined by (36) and (37) remains valid except for unknown scale. Scale was arbitrarily set to Chu's value of $0.166\lambda^2$ for the backscatter point $\beta = 0$; this operation was equivalent to assuming $z_{\text{rad}} \sin^2(\pi L/\lambda) = 224.6$ Ω in the model.

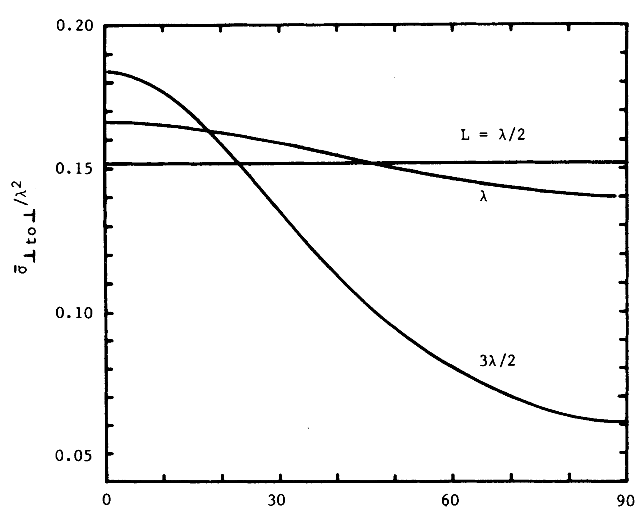

Fig. 3. Spherically averaged bistatic cross sections for linear transmitting and receiving polarizations perpendicular to scattering plane. Cross sections have even symmetry about $\beta = \pi/2$ (90°) and $\beta = \pi$ (180°).

[3] z_{rad} required in (39) is set once L/λ is chosen.

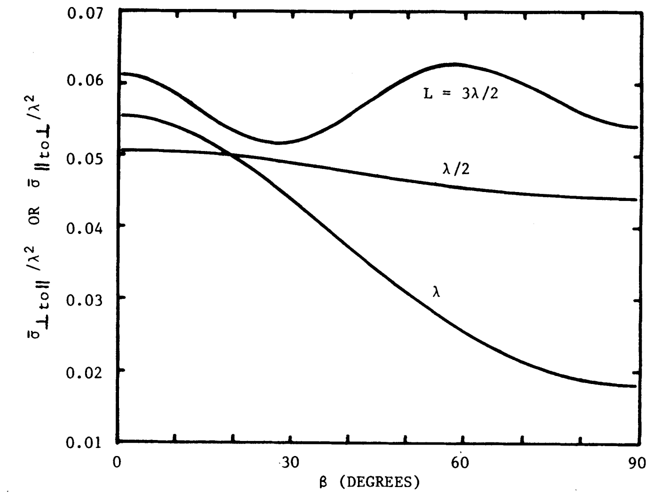

Fig. 4. Spherically averaged bistatic cross sections for linear transmitting and receiving polarizations, one perpendicular to and one parallel with scattering plane. Cross sections have even symmetry about $\beta = \pi/2$ (90°) and $\beta = \pi$ (180°).

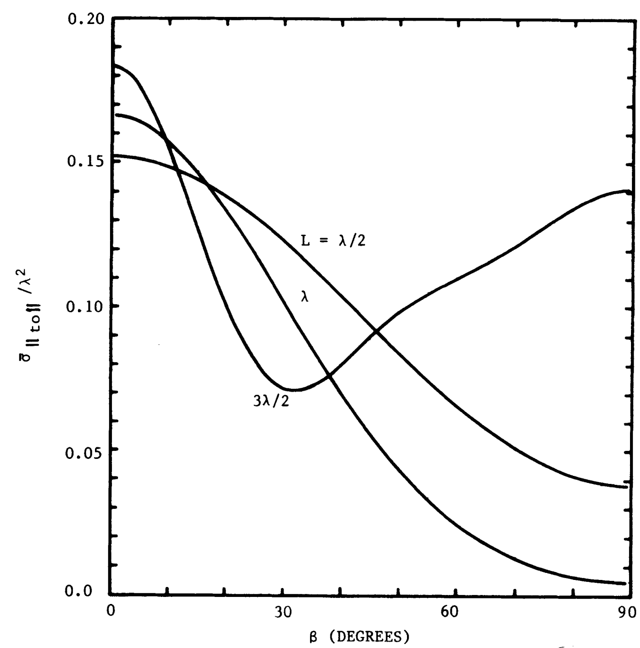

Fig. 5. Spherically averaged bistatic cross sections for linear transmitting and receiving polarizations parallel to scattering plane. Cross sections have even symmetry about $\beta = \pi/2$ (90°) and $\beta = \pi$ (180°).

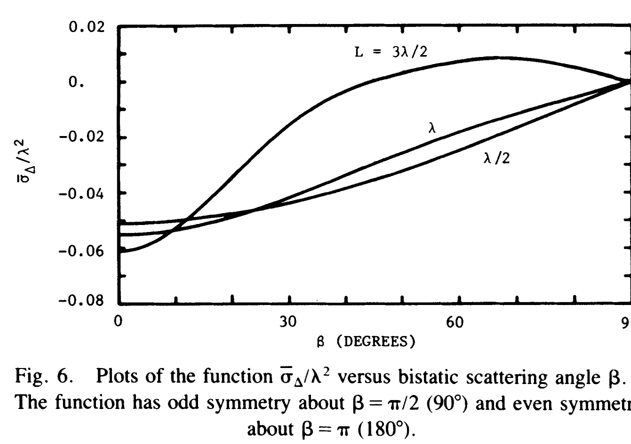

Fig. 6. Plots of the function $\bar{\sigma}_{\Delta}/\lambda^2$ versus bistatic scattering angle β. The function has odd symmetry about $\beta = \pi/2$ (90°) and even symmetry about $\beta = \pi$ (180°).

Data for $L = \lambda/2$ agree well with those of Mack and Reiffen [21]. Data for $L = \lambda$ do not agree with those in [21] because of an error recently confirmed by Reiffen [37]; the error appears to stem from an erroneous equation [21, (10)] used in computer simulation. The error has apparently never been corrected in the literature and it has been propagated [6, p. 302].

E. Relationship to Stokes Parameter Method

As mentioned above, the analysis of Dedrick et al. [30] using Stokes parameters showed that only four parameters denoted by $\langle\sigma M_{11}\rangle$, $\langle\sigma M_{12}\rangle$, $\langle\sigma M_{22}\rangle$, and $\langle\sigma M_{33}\rangle$ are needed to find cross sections for any polarizations of transmission and reception. Unfortunately, their work related to polarizations defined with respect to the scattering plane, and general relations for geometry such as in Fig. 1 were not developed. Also their evaluations of the four functions were not done for the usual resonant dipole lengths. Furthermore, their numerical work relied on a computer integration method that produced significant error (observe fluctuations in their plotted data). We can show that these difficulties are all overcome by use of the present results. The procedure is simply to show how the four functions of [30] are related to the four cross sections found here to be required for the general problem.

Parameters $\bar{\sigma}_{\parallel \text{ to } \parallel}$, $\bar{\sigma}_{\perp \text{ to } \perp}$, and $\bar{\sigma}_{\parallel \text{ to } \perp} = \bar{\sigma}_{\perp \text{ to } \parallel}$ here and the respective parameters $\sigma_{\parallel \text{ to } \parallel}$, $\sigma_{\perp \text{ to } \perp}$, and $\sigma_{\parallel \text{ to } \perp}$ of [30] are defined identically. Thus, we use the equalities and solve equation (19) of [30] to obtain

$$\langle\sigma M_{11}\rangle = \frac{1}{2}(\bar{\sigma}_{\parallel \text{ to } \parallel} + 2\bar{\sigma}_{\perp \text{ to } \parallel} + \bar{\sigma}_{\perp \text{ to } \perp}) \tag{50}$$

$$\langle\sigma M_{22}\rangle = \frac{1}{2}(\bar{\sigma}_{\parallel \text{ to } \parallel} - 2\bar{\sigma}_{\perp \text{ to } \parallel} + \bar{\sigma}_{\perp \text{ to } \perp}) \tag{51}$$

$$\langle\sigma M_{12}\rangle = \frac{1}{2}(\bar{\sigma}_{\parallel \text{ to } \parallel} - \bar{\sigma}_{\perp \text{ to } \perp}). \tag{52}$$

To show the remaining relationship, let $\bar{\sigma}_{/\text{to}/}$ denote the value of $\bar{\sigma}$ corresponding to linear transmitted and received preferred polarizations tilted 45° from the respective ϕ_T and ϕ_R axes when T, D, and R all lie in the x,y plane of Fig. 1. For the same conditions denote the value of $\bar{\sigma}_x$ by $\bar{\sigma}_{/\text{to}\backslash}$. Then it can be shown that

$$\langle\sigma M_{33}\rangle = \bar{\sigma}_{/\text{to}/} - \bar{\sigma}_{/\text{to}\backslash}\; 2\bar{\sigma}_{\Delta}. \tag{53}$$

IV. MULTIPLE DIPOLE SCATTERING

When scattering is due to many, say N, dipoles in a cloud the received fields are the sums of fields caused by individual dipoles.[4] For a typical, say ith, dipole, (22) again applies, where now all the parameters of $[R]$, $[d]$, $[T]$, Q_T, and even E_T may in general depend on i.

[4]We shall assume that scattered fields due to multiple reflections between dipoles are negligible.

However, some reasonable assumptions will greatly simplify the developments. Let us assume the dipoles viewed by the transmitter are either far enough away or are of sufficiently small range and angular extent that their incident waves are all of the same polarization and all of about the same field strength ($1/r_1$ factor about the same for all dipoles). These assumptions allow $|E_T|$, Q_T, and $[T]$ to all be approximately independent of i. By making similar assumptions about the cloud–receiver path, $[R]$ is approximately independent of i. These assumptions basically make (4) and (5) valid provided $|E_{R_1}|^2$ and $|E_{R_2}|^2$ are properly determined; alternatively, (23) and (24) are equivalent valid forms.

The, now total, received field "amplitude" components, denoted again by E_{R_1} and E_{R_2}, from (22) are now[5]

$$\begin{bmatrix} E_{R_1} \\ E_{R_2} \end{bmatrix} =$$

$$\frac{1}{1 + |Q_R|^2} \begin{bmatrix} 1 & Q_R^* \\ -Q_R & 1 \end{bmatrix} [R]\,[D]\,[T] \begin{bmatrix} 1 \\ Q_T \end{bmatrix} |E_T| \tag{54}$$

where all terms are defined as before except

$$[D] \triangleq \begin{bmatrix} D_{11} & D_{12} \\ D_{21} & D_{22} \end{bmatrix} \tag{55a}$$

where

$$D_{mn} = \sum_{i=1}^{N} d_{mni} \exp(-j2\pi r_{1i}/\lambda), \qquad m \text{ and } n = 1, 2. \tag{55b}$$

Parameters d_{mni} for m and $n = 1, 2$, are now given by (38) with variables θ_d and ϕ_d replaced by θ_{di} and ϕ_{di}, respectively. Variable r_2 in the exponent of (39) is replaced by r_{2i}, but, because of the above assumptions, r_2 in the factor $1/r_2$ remains the nominal distance to the cloud and does not depend on i.

The procedure for finding $\bar{\sigma}$ and $\bar{\sigma}_x$ proceeds exactly as above for one dipole; we expand (54) and obtain $|E_{R_1}|^2$ and $|E_{R_2}|^2$ so that substitution into (23) and (24) can be made. The expansions again lead to 10 functions as given in (44) except where D_{mn} replaces d_{mn}, m and $n = 1, 2$. Expectations now must include the randomness of dipole positions because positions affect the phases of

[5]The phase of E_T has been incorporated into the definition of $[D]$.

the parameters D_{mn} through factors $\exp[-j2\pi(r_{1i} + r_{2i})/\lambda]$. By making the reasonble assumption that the phases $2\pi(r_{1i} + r_{2i})/\lambda$ are uniformly distributed on $(0, 2\pi)$ and that dipole phases are independent, due to independent positions, we find the important result that the 10 functions of (44) involving D_{mn} are individually equal to the 10 functions of (44) involving d_{mn} for a single dipole multiplied by N. Thus all cross sections based on scattering from the N dipoles are equal simply to N times the cross section of a typical dipole. Dipole cloud cross sections are simply N times the results for one dipole which leads finally to (6) and (7).

V. SCATTERING EXAMPLES

A. Transmitter–Cloud–Receiver in x,y Plane

Several examples serve to illustrate the physical meanings of $\bar{\sigma}_{\perp \text{ to } \perp}$, $\bar{\sigma}_{\perp \text{ to } \parallel}$, $\bar{\sigma}_{\parallel \text{ to } \parallel}$, and $\bar{\sigma}_{\Delta}$. These examples assume the transmitter, the receiver, and the cloud's centroid to lie in the x,y plane (Fig. 1). Thus $\theta_1 = \pi/2$, $\theta_2 = \pi/2$, $\beta = \phi_2 - \phi_1 - \pi$ and, from (8)–(15), we find $T_1 = 1$, $T_2 = 0$, $R_1 = 1$, and $R_2 = 0$ so $X_1 = 1$, $X_2 = Q_T$, $W_1 = 1$, and $W_2 = Q_R$. The reduced forms of (6) and (7) become

$$\bar{\sigma} = \frac{N}{(1 + |Q_T|^2)(1 + |Q_R|^2)} \Big\{ \bar{\sigma}_{\perp \text{ to } \perp} + \bar{\sigma}_{\perp \text{ to } \parallel}(|Q_R|^2 + |Q_T|^2) + \bar{\sigma}_{\parallel \text{ to } \parallel}|Q_R|^2|Q_T|^2 + 4\bar{\sigma}_{\Delta}\,\mathrm{Re}(Q_R)\,\mathrm{Re}(Q_T) \Big\} \tag{56}$$

$$\bar{\sigma}_x = \frac{N}{(1 + |Q_T|^2)(1 + |Q_R|^2)} \Big\{ \bar{\sigma}_{\perp \text{ to } \parallel}(1 + |Q_T|^2|Q_R|^2) + \bar{\sigma}_{\perp \text{ to } \perp}|Q_R|^2 + \bar{\sigma}_{\parallel \text{ to } \parallel}|Q_T|^2 - 4\bar{\sigma}_{\Delta}\,\mathrm{Re}(Q_R)\,\mathrm{Re}(Q_T) \Big\}. \tag{57}$$

A transmitter or receiver having vertical (V) linear polarization has its electric field vector perpendicular ($\perp$) to the scattering plane, while horizontal (H) linear corresponds to a field vector parallel ($\parallel$) to the scattering plane.

Example 1. Transmit V, receive V: From Table I, $Q_T = 0$, $Q_R = 0$. From (56), the cross section, denoted by $\bar{\sigma}_{VV}$, for the preferred receive polarization is

$$\bar{\sigma}_{VV} \triangleq \bar{\sigma} = N\bar{\sigma}_{\perp \text{ to } \perp}. \tag{58}$$

The cross polarization corresponds to reception of H:

$$\bar{\sigma}_{VH} \triangleq \bar{\sigma}_x = N\bar{\sigma}_{\perp \text{ to } \parallel} \tag{59}$$

from (57).

Example 2. Transmit H, receive H: From Table I, $Q_T = \infty$, $Q_R = \infty$. From (56) cross section, $\bar{\sigma}_{HH}$ is

$$\bar{\sigma}_{HH} \triangleq \bar{\sigma} = N\bar{\sigma}_{\parallel \text{ to } \parallel}. \tag{60}$$

Cross polarization $\bar{\sigma}_{HV}$, from (57) becomes

$$\bar{\sigma}_{HV} \triangleq \bar{\sigma}_x = N\bar{\sigma}_{\perp \text{ to } \parallel} = N\bar{\sigma}_{\parallel \text{ to } \perp}. \tag{61}$$

Example 3. Transmit V, receive H: Here $Q_T = 0$, $Q_R = \infty$. Cross sections from (56) and (57), denoted by $\bar{\sigma}_{VH}$ and $\bar{\sigma}_{VV}$, become

$$\bar{\sigma}_{VH} \triangleq \bar{\sigma} = N\bar{\sigma}_{\perp \text{ to } \parallel} \tag{62}$$

$$\bar{\sigma}_{VV} \triangleq \bar{\sigma}_x = N\bar{\sigma}_{\perp \text{ to } \perp}. \tag{63}$$

Example 4. Transmit H, receive V: Here $Q_T = \infty$, $Q_R = 0$. Similarly, to Example 3, we get

$$\bar{\sigma}_{HV} \triangleq \bar{\sigma} = N\bar{\sigma}_{\perp \text{ to } \parallel} = N\bar{\sigma}_{\parallel \text{ to } \perp} \tag{64}$$

$$\bar{\sigma}_{HH} \triangleq \bar{\sigma}_x = N\bar{\sigma}_{\parallel \text{ to } \parallel}. \tag{65}$$

Example 5. Transmit linear tilted from horizontal by 45°, receive is the same. Here $Q_T = 1$, $Q_R = 1$. Denote by $N\bar{\sigma}_{\diagup \text{to} \diagup}$ the total cross section applicable to the preferred receiver polarization given by (56). It is

$$N\bar{\sigma}_{\diagup \text{to} \diagup} \triangleq \bar{\sigma} = \frac{N}{4}[\bar{\sigma}_{\perp \text{ to } \perp} + 2\bar{\sigma}_{\perp \text{ to } \parallel} + \bar{\sigma}_{\parallel \text{ to } \parallel} + 4\bar{\sigma}_{\Delta}]. \tag{66}$$

The cross section, denoted by $N\bar{\sigma}_{\diagup \text{to} \diagdown}$, for the receiver cross polarization given by $\bar{\sigma}_x$ is

$$N\bar{\sigma}_{\diagup \text{to} \diagdown} \triangleq \bar{\sigma}_x = (N/4)[\bar{\sigma}_{\perp \text{ to } \perp} + 2\bar{\sigma}_{\perp \text{ to } \parallel} + \bar{\sigma}_{\parallel \text{ to } \parallel} - 4\bar{\sigma}_{\Delta}]. \tag{67}$$

By subtracting (67) from (66), we get

$$\bar{\sigma}_{\Delta} = (\bar{\sigma}_{\diagup \text{to} \diagup} - \bar{\sigma}_{\diagup \text{to} \diagdown})/2. \tag{68}$$

Thus $\bar{\sigma}_{\Delta}$ is half the difference in cross sections (per dipole) seen by the receiver in preferred and orthogonal polarizations when transmit and preferred receiver polarizations are linear and tilted 45° with respect to the scattering plane.

By retracing this example, we also find

$$\bar{\sigma}_{\Delta} = (\bar{\sigma}_{\diagdown \text{to} \diagdown} - \bar{\sigma}_{\diagdown \text{to} \diagup})/2. \tag{69}$$

Example 6. Transmit right circular, denoted by O_R, receive right circular. Here $Q_T = -j$, $Q_R = -j$, and

$$\bar{\sigma}_{O_R \text{ to } O_R} \triangleq \bar{\sigma} = (\bar{\sigma}_{\perp \text{ to } \perp} + 2\bar{\sigma}_{\perp \text{ to } \parallel} + \bar{\sigma}_{\parallel \text{ to } \parallel})\,N/4 \tag{70}$$

$$\bar{\sigma}_{O_R \text{ to } O_L} \triangleq \bar{\sigma}_x = \bar{\sigma}_{O_R \text{ to } O_R} \tag{71}$$

where O_L denotes left circular. Here we see that a circularly polarized receiver sees the same cross section regardless of choice of rotation sense. Similarly, it results that

$$\overline{\sigma}_{O_L \text{ to } O_L} \triangleq \overline{\sigma} = (\overline{\sigma}_{\perp \text{ to } \perp} + 2\overline{\sigma}_{\perp \text{ to } \parallel} + \overline{\sigma}_{\parallel \text{ to } \parallel}) N/4 \tag{72}$$

$$\overline{\sigma}_{O_L \text{ to } O_R} \triangleq \overline{\sigma}_x = \overline{\sigma}_{O_L \text{ to } O_L}. \tag{73}$$

Thus bistatic cross section is the same when both transmitter and receiver have circular polarizations, regardless of combinations of rotation senses.

B. Cloud–Receiver Not in x,y Plane (Example 7)

As a final example, let the transmitter have linear polarization in the θ_1 direction ($Q_T = 0$) and the receiver preferred polarization be linear in the θ_2 direction ($Q_R = 0$). Let the centroid of a cloud of half-wave dipoles be located at $\theta_1 = 25\pi/180$ (or 25°) and $\phi_1 = 75\pi/180$ (or 75°) at a distance $r_1 = 5(10^3)$ m. The receiver is at a distance $r_2 = 10^4$ m from the cloud centroid and a distance of $12.5(10^3)$ m from the transmitter. The receiver has an elevation angle of 50° from the x,y plane as seen from the transmitter. We find bistatic cross sections $\overline{\sigma}/(N\lambda^2)$ and $\overline{\sigma}_x/(N\lambda^2)$.

From simple geometry as in Fig. 1, we find that $\beta = 108.21\pi/180$ (or 108.21°), $\theta_2 = 59.71\pi/180$, $\phi_2 = 321.65\pi/180$, and $\phi_1 - \phi_2 = 113.35\pi/180$. From (8)–(15) we calculate $X_1 = T_1 = 0.835$, $X_2 = T_2 = 0.551$, $W_1 = R_1 = 0.408$, and $W_2 = R_2 = -0.913$. From Figs. 3–6 or the tables in [36], at scattering angle 71.79° [90.0° − (108.21° − 90.0°)] we find $\overline{\sigma}_{\parallel \text{ to } \parallel}/\lambda^2 = 0.04918$, $\overline{\sigma}_{\perp \text{ to } \perp}/\lambda^2 = 0.15116$, $\overline{\sigma}_{\perp \text{ to } \parallel}/\lambda^2 = 0.04464$, and $\overline{\sigma}_{\Delta}/\lambda^2 = 0.01151$. Finally, from (6) and (7), we calculate $\overline{\sigma}/(N\lambda^2) = 0.0503$ and $\overline{\sigma}_x/(N\lambda^2) = 0.1146$. Note for this problem's geometry the antenna with preferred polarization would receive less power than one with the orthogonal polarization.

VI. SUMMARY AND DISCUSSION

In this paper the spherically averaged bistatic cross sections applicable to a cloud of randomly positioned and randomly oriented resonant dipoles have been found. For a transmitting antenna of arbitrarily specified polarization (set by parameter Q_T as discussed in the Appendix), a receiving antenna of arbitrarily specified (by parameter Q_R) polarization, and geometry shown in Fig. 1, the cross section is given by $\overline{\sigma}$ of (6). Cross section applicable to the corresponding orthogonal receive antenna polarization is given by $\overline{\sigma}_x$ of (7).

Parameters X_1, X_2, W_1, and W_2 depend on the geometry of the problem and are found from (8)–(15). The functions $\overline{\sigma}_{\perp \text{ to } \perp}$, $\overline{\sigma}_{\perp \text{ to } \parallel}$, $\overline{\sigma}_{\parallel \text{ to } \parallel}$, and $\overline{\sigma}_{\Delta}$ depend on the length of the resonant dipole chosen (half-wavelength, full-wavelength, etc.) and on the scattering angle β of Fig. 1; they are plotted in Figs. 3–6 and tabularized in [36].

Our results agree well with [21] for half-wavelength dipoles, correct erroneous results in [21] for full-wave dipoles, give new results for three-halves wavelength dipoles, and have produced explicit expressions for cross sections for any geometry. The relationships to another analysis method using Stokes parameters [30] has been shown, and, by proper use of the parameters given in this paper, the parameters of [30] may be computed with better accuracy.

Equations (6) and (7) were derived assuming perfectly conducting, thin dipoles of resonant length, having a sunusoidal current distribution along their length. Such a distribution is reasonable for shorter wire lengths; it becomes questionable for longer lengths. The model used is therefore probably not applicable for lengths longer than about three-halves wavelength.

APPENDIX. POLARIZATION CONSIDERATIONS

A general, elliptically polarized plane wave propagating in the r direction has electric field components E_θ and E_ϕ in the θ and ϕ directions at the origin of a spherical coordinate system given by [34]

$$E_\theta = A \cos \omega t = \mathrm{Re}(A\, e^{j\omega t}) \tag{A1}$$

$$E_\phi = B \cos(\omega t + \alpha) = \mathrm{Re}(B\, e^{j\omega t + j\alpha}). \tag{A2}$$

Here A and B are peak amplitudes (positive quantities), α is a phase angle, ω is angular frequency, and t is time. The wave is completely specified by the three quantities A, B, and α. For an observer at the origin looking in the direction of propagation, the instantaneous electric field vector appears to rotate in a counterclockwise direction for $0 < \alpha < \pi$ regardless of the relative amplitudes of A and B; this is defined as left-elliptical polarization by IEEE standards. For $-\pi < \alpha < 0$, rotation is clockwise and we have right-elliptical polarization. If $A = B$ the locus of the tip of the electric field vector is a circle when $\alpha = \pm\,\pi/2$; rotation is counterclockwise for $\alpha = \pi/2$ and the wave polarization is called left circular, for $\alpha = -\pi/2$ we have clockwise rotation and right-circular polarization.

Polarization Ellipses

The ellipse traced by the electric field vector is illustrated in Fig. 7 (note that positive θ and ϕ directions are downward and left, respectively).

Polarization can also be defined by the three quantities shown: a and b are ellipse minor and major axes half-lengths, respectively; δ is the tilt of the major axis from the ϕ axis. It can be shown that A, B, and α are related to a, b, and δ by

$$a^2 = \frac{2A^2B^2 \sin^2 \alpha}{(A^2+B^2) - \sqrt{(A^2+B^2)^2 - 4A^2B^2 \sin^2 \alpha}} \tag{A3}$$

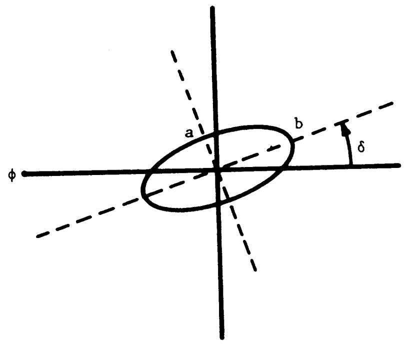

Fig. 7. Locus of tip of electric field vector for elliptical polarization.

$$b^2 = \frac{2A^2B^2 \sin^2 \alpha}{(A^2+B^2) + \sqrt{(A^2+B^2)^2 - 4A^2B^2 \sin^2 \alpha}} \tag{A4}$$

$$\tan 2\delta = \frac{2AB \cos \alpha}{B^2 - A^2}. \tag{A5}$$

The ratio a/b is often called axial ratio and is usually specified as a number greater than unity. Thus if $a/b < 1$, the axial ratio becomes b/a.

The reverse relationships are

$$A^2 = a^2 \sin^2 \delta + b^2 \cos^2 \delta \tag{A6}$$

$$B^2 = a^2 \cos^2 \delta + b^2 \sin^2 \delta \tag{A7}$$

$$\tan \alpha = \frac{2ab}{(a^2 - b^2) \sin 2\delta}. \tag{A8}$$

Complex Fields and Wave Decomposition

In the text, fields are represented by complex quantities. The complex field components are the exponential extensions of (A1) and (A2), that is, E_θ is represented as the complex quantity $A \exp(j\omega t)$. Usually the common factor $\exp(j\omega t)$ is suppressed since this carries through all steps in analysis. The remaining factor is called the complex envelope of the field. With these points in mind, fields in the text are complex with components

$$E_\theta = A \tag{A9}$$

$$E_\phi = B\, e^{j\alpha}. \tag{A10}$$

In vector (matrix) notation these components give

$$\begin{bmatrix} E_\theta \\ E_\phi \end{bmatrix} = \begin{bmatrix} A \\ AQ \end{bmatrix} = A \begin{bmatrix} 1 \\ Q \end{bmatrix} \tag{A11}$$

where we define a field component ratio,[6] denoted by Q, as

$$Q \triangleq E_\phi / E_\theta = B\, e^{j\alpha}/A. \tag{A12}$$

Table I illustrates values of Q for some typical wave polarizations.

[6]This ratio has also been called a "polarization factor" in [38] and given a symbol different than Q.

If (A11) represents electric field vector $\boldsymbol{E}$, the magnitude squared of $\boldsymbol{E}$ is

$$|\boldsymbol{E}|^2 = [E_\theta^* \quad E_\phi^*] \begin{bmatrix} E_\theta \\ E_\phi \end{bmatrix} = |E_\theta|^2 + |E_\phi|^2$$
$$= |A|^2[1 + |Q|^2]. \tag{A13}$$

Next, let $\boldsymbol{E}$ represent an arbitrarily polarized field given by (A11) and let two other elliptically polarized waves be described by

$$\boldsymbol{E}_1 = \begin{bmatrix} A_1 \\ A_1 Q_1 \end{bmatrix}, \qquad \boldsymbol{E}_2 = \begin{bmatrix} A_3 \\ A_2 \end{bmatrix}. \tag{A14}$$

We show that $\boldsymbol{E}$ can be decomposed into the sum of $\boldsymbol{E}_1$, having an arbitrary (selected) elliptical polarization set by Q_1, and $\boldsymbol{E}_2$, having an elliptical polarization orthogonal to that of $\boldsymbol{E}_1$. Since $\boldsymbol{E}_1$ and $\boldsymbol{E}_2$ are to be orthogonal, their inner product is zero and

$$\boldsymbol{E}_1 \cdot \boldsymbol{E}_2 = [A_1^* \quad A_1^* Q_1^*] \begin{bmatrix} A_3 \\ A_2 \end{bmatrix}$$
$$= A_1^* A_3 + A_1^* Q_1^* A_2 = 0 \tag{A15}$$

which requires $A_3 = -A_2 Q_1^*$ for any A_2. Thus we require

$$\boldsymbol{E} = \begin{bmatrix} A \\ AQ \end{bmatrix} = \boldsymbol{E}_1 + \boldsymbol{E}_2 = \begin{bmatrix} A_1 \\ A_1 Q_1 \end{bmatrix} + \begin{bmatrix} -A_2 Q_1^* \\ A_2 \end{bmatrix}$$
$$= \begin{bmatrix} A_1 - A_2 Q_1^* \\ A_1 Q_1 + A_2 \end{bmatrix}$$
$$= \begin{bmatrix} 1 & -Q_1^* \\ Q_1 & 1 \end{bmatrix} \begin{bmatrix} A_1 \\ A_2 \end{bmatrix} \tag{A16}$$

After solving (A16) for A_1 and A_2 we have

$$A_1 = \frac{A(1 + QQ_1^*)}{1 + |Q_1|^2} \tag{A17}$$

$$A_2 = \frac{A(Q - Q_1)}{1 + |Q_1|^2}. \tag{A18}$$

These results show that any elliptically polarized wave can be decomposed into the sum of one elliptically polarized field of specified polarization and amplitude given by (A17) and another wave with amplitude given by (A18) with polarization orthogonal to the specified wave. This means any received wave can be separated into the component to which a given antenna responds plus another component to which it does not respond.

Finally, we note that the powers in the two received waves are proportional to $|\boldsymbol{E}_1|^2$ and $|\boldsymbol{E}_2|^2$

$$|\boldsymbol{E}_1|^2 = |A_1|^2(1 + |Q_1|^2) \tag{A19}$$

$$|\boldsymbol{E}_2|^2 = |A_2|^2(1 + |Q_1|^2). \tag{A20}$$

ACKNOWLEDGMENT

The author is grateful to Prof. R.C. Johnson of the University of Florida for several helpful discussions.

REFERENCES

[1] Fink, D.G. (1946)
Radar countermeasures.
Electronics, 19 (Jan. 1946), 92–97.

[2] DilPare, A.L. (1970)
Chaff primer.
Microwaves, 9, 12 (Dec. 1970), 46–47.

[3] Puskar, R.J. (1974)
Radar reflector studies.
In *Proceedings of the IEEE 1974 National Aerospace and Electronics Conference* (May 13–15, 1974), pp. 177–183.

[4] Sundaram, G.S. (1976)
Expendables in electronic warfare—Proven decoys for survival.
International Defense Review (Dec. 1976), 1045–1050.

[5] Butters, B.C.F. (1982)
Chaff.
IEEE proceedings, 129, pt. F3, (June 1982), 197–201.

[6] Ruck, G.T. (Ed.) (1970)
Radar Cross Section Handbook, vol. 1.
New York: Plenum Press, 1970.

[7] Peebles, P.Z., Jr. (1983)
Radar chaff: A bibliography.
University of Florida Report HDL-CR-83-107-5 for Harry Diamond Laboratories (U.S. Army) Adelphi, MD 20783, Nov. 1983.

[8] Bloch, F., Hamermesh, M. and Phillips, M. (1944)
Return cross sections from random oriented resonant half-wave length chaff.
Radio Research Laboratory, Harvard University, Cambridge, Mass., Technical memorandum 411-TM-127, June 19, 1944.

[9] Van Vleck, J.H., Bloch, F., and Hamermesh, M. (1947)
Theory of radar reflection from wires or thin metallic strips.
Journal of Applied Physics, 18 (March 1947), 274–294.

[10] King, R., and Middleton, D. (1946)
The cylindrical antenna: Current and impedance.
Quarterly of Applied Mathematics, 3, 4 (1946), 302–335.

[11] Tai, C.T. (1952)
Electromagnetic back-scattering from cylindrical wires.
Journal of Applied Physics, 23 (Aug. 1952), 909–916.,

[12] Cassedy, E.S., and Fainberg, J. (1960)
Back scattering cross sections of cylindrical wires of finite conductivity.
IRE Transactions on Antennas and Propagation, AP-8, 1 (Jan. 1960), 1–7.

[13] Harrison, C.W., Jr., and Heinz, R.O. (1963)
On the radar cross section of rods, tubes, and strips of finite conductivity.
IEEE Transactions on Antennas and Propagation, AP-11, 4 (July 1963), 459–468.

[14] Chen, C.-L. (1968)
On the scattering of electromagnetic waves from a long wire.
Radio Science, 3 (new series), 6 (June 1968), 585–598.

[15] Wickliff, R.G., and Garbacz, R.J. (1974)
The average backscattering cross section of clouds of randomized resonant dipoles.
IEEE Transactions on Antennas and Propagation, AP-22, 3 (May 1974), 503–505; see also corrections in *AP-22,* 6 (Nov. 1974), 842–843.

[16] Medgyesi-Mitschang, L.N., and Eftimiu, C. (1982)
Scattering from wires and open circular cylinders of finite length using entire domain Galerkin expansions.
IEEE Transactions on Antennas and Propagation, AP-30, 4 (July 1982), 628–636.

[17] Pyati, V.P. (1975)
On the convergence of the scattering statistics of finite number of randomly oriented dipoles to Rayleigh.
Proceedings of the IEEE, 63, 6 (June 1975), 985–986.

[18] Wong, J.L., Reed, I.S., and Kaprielian, Z.A. (1967)
A model for the radar echo from a random collection of rotating dipole scatterers.
IEEE Transactions on Aerospace and Electronic Systems, AES-2, 2 (Mar. 1967), 171–178.

[19] Ioannidis, G.A. (1979)
Model for spectral and polarization characteristics of chaff.
IEEE Transactions on Aerospace and Electronic Systems, AES-15, 5 (Sept. 1979), 723–726.

[20] Hessemer, R.A., Jr. (1961)
Scatter communications with radar chaff.
IRE Transactions on Antennas and Propagation, AP-9, 2 (Mar. 1961), 211–217.

[21] Mack, C.L., Jr., and Reiffen, B. (1964)
RF characteristics of thin dipoles.
Proceedings of the IEEE, 52, 5 (May 1964), 533–542.

[22] Harrington, R.F. (1964)
RF characteristics of thin dipoles.
Proceedings of the IEEE, 52, 12 (Dec. 1964), 1736–1737.

[23] Borison, S.L. (1967)
Bistatic scattering cross section of a randomly oriented dipole.
IEEE Transactions on Antennas and Propagation, AP-15, 2 (Mar. 1967), 320–321.

[24] Palermo, C.J. and Bauer, L.H. (1965)
Bistatic scattering cross section of chaff dipoles with applications to communications.
Proceedings of the IEEE, 53, 8 (Aug. 1965), 1119–1121.

[25] DiCaudo, V.J., and Martin, W.W. (1966)
Approximate solution to bistatic radar cross section of finite length, infinitely conducting cylinder.
IEEE Transactions on Antennas and Propagation, AP-14, 5 (Sept. 1966), 668–669.

[26] Harrington, R.F., and Mautz, J.R. (1967)
Straight wires with arbitrary excitation and loading.
IEEE Transactions on Antennas and Propagation, AP-15, 4 (July 1967), 502–515.

[27] Breithaupt, R.W. (1967)
Bistatic scattering by a thin, lossy cylindrical wire.
Canadian Journal of Physics, 45, 6 (June 1967), 1965–1980.

[28] Einarsson, O. (1969)
Electromagnetic scattering by a thin finite wire.
Acta Polytechnica Scandinavica, Electrical Engineering Series 23, UDC 538.566, 621.396.67, Stockholm, May 1969.

[29] Garbacz, R.J., Cable, V., Wickliff, R., Caldecott, R., Buk, J., Lam, D., Demarest, K., and Yee, A. (1975)
Advanced radar reflector studies.
Report AFAL-TR-75-219, Electroscience Laboratory, Ohio State University, Columbus, Dec. 1975; also DTIC Document ADB013005.

[30] Dedrick, K.G., Hessing, A.R., and Johnson, G.L. (1978)
Bistatic radar scattering by randomly oriented wires.
IEEE Transactions on Antennas and Propagation, AP-26, 3 (May 1978), 420–426.

[31] Heath, G.E. (1981)
Bistatic scattering reflection asymmetry, polarization reversal asymmetry, and polarization reversal reflection symmetry.
IEEE Transactions on Antennas and Propagation, AP-29, 3 (May 1981), 429–434.

[32] Heath, G.E. (1981)
Properties of the linear polarization bistatic scattering matrix.
IEEE Transactions on Antennas and Propagation, AP-29, 3 (May 1981), 523–525.

[33] FitzGerrell, R.G. (1965)

Radiation efficiencies of half-wave dipole antennas.
IEEE Transactions on Antennas and Propagation, AP-13, 2 (Mar. 1965), 326–327.

[34] Kraus, J.D. (1950)
Antennas.
New York: McGraw-Hill, 1950.

[35] Cross, J.L. (1969)
Response of arrays to stochastic fields.
Ph.D. dissertation, University of Florida, Gainesville, 1969.

[36] Peebles, P.Z., Jr. (1983)
Bistatic radar cross sections of chaff.
University of Florida Report HDL-CR-83-107-6 for Harry Diamond Laboratories (U.S. Army) Adelphi, MD 20783, June 1983.

[37] Reiffen, B., private communication, June 1983.

[38] Beckmann, P., and Spizzichino, A. (1963)
The Scattering of Electromagnetic Waves from Rough Surfaces.
New York: MacMillan, 1963.

Peyton Z. Peebles, Jr. (S'56–M'58–SM'76) was born in Columbus, Ga., on September 10, 1934. He received the B.S. degree in 1957 from Evansville College, Evansville, Ind., the M.S. degree in 1963 from Drexel Institute of Technology, Philadelphia, Pa., and the Ph.D. degree in 1967 from the University of Pennsylvania, Philadelphia.

Except for a brief service period, he worked for RCA from 1957 to 1969, where he was involved primarily in radar system analysis. From 1969 to 1981 he taught at the University of Tennessee, except from 1976 to 1977, when he was a Visiting Professor at the University of Hawaii, Honolulu. He is now a Professor of Electrical Engineering at the University of Florida, Gainesville, where his principal research interests relate to radar and communication systems. He has authored or coauthored 45 technical papers and is the author of two books, *Communication System Principles* (1976) and *Probability, Random Variables, and Random Signal Principles* (1980).

Dr. Peebles is a member of Tau Beta Pi, Eta Kappa Nu, Sigma Xi, Sigma Pi Sigma, and Phi Beta Chi.